EXPERIMENTAL AND NUMERICAL INVESTIGATION OF AERODYNAMIC INTERACTIONS ON A TILT-ROTOR CONFIGURATION

C. Barla[1], T. Lefebvre[2], E. Berton[1], P. Beaumier[2], D. Favier[1]

[1]Laboratory of Aerodynamic and Biomechanics of Motion,
USR 2164 CNRS & University of Méditerranée
163 Avenue de Luminy, CP 918, 13288 Marseille cedex 09, France
E-mail: charlie.barla@univmed.fr

[2] ONERA
BP72, 29 Avenue de la Division Leclerc, 92322 Chatillon Cedex, France
E-mail: thierry.lefebvre@onera.fr

Key words: Aerodynamic Interactions, Tilt-Rotor, Hover and Cruise Flight.

Abstract: This paper concerns a collaborative research work between LABM and ONERA research center. It focuses on aerodynamic interactions occurring on a tilt-rotor configuration in three different flight conditions (hover, transition and cruise). The present study concerns both an experimental investigation conducted in the S1L wind-tunnel at LABM combined with numerical investigations mainly based on a comprehensive analysis (HOST code) done by ONERA for the same tilt-rotor and flight configurations. Numerical and experimental results are compared in order to validate the numerical models. Experiments are carried out on a three bladed rotor coupled with a fixed flapped wing placed in the wake of the rotor. The main aim of this study is to characterize and quantify the global and local aerodynamic interactions features as a function of different parametric flight conditions. To this end, global performance (Z_b: rotor lift, C_T: rotor thrust, C_Q: rotor torque coefficients) have been firstly measured on the isolated rotor as a function of collective pitch angle θ in order to characterize the rotor itself in different flight configurations. The aerodynamic coefficients of the isolated wing (C_L, C_D, C_M) have been also determined and finally, the performance of each component placed at the same time in the wind tunnel have been measured in order to highlight the influence of the wing on rotor performance and vice versa. Thanks to this database the evolution of the download effect on the wing can be studied: this phenomenon appears to be more pronounced in hovering flight than in transition flight. Moreover, some local aerodynamic performance will be determined like rotor tip vortex paths or pressure coefficients directly measured on the wing to study the evolution of the wake and the deflection due to the presence of the wing in the rotor wake.

1 INTRODUCTION

During the two previous decades, new propulsion concepts (including tilting rotors or tilting wings) have been improved in aeromechanic performance in order to decrease not only aerodynamic interactions but also acoustic and vibratory levels [1]. Nevertheless, the integration of the propulsive system and its influence on its nearest environment (wing, nacelle, airframe, etc…) still remains a restrictive factor in the optimization of this new kind of concept. Indeed, the tilt-rotor configuration is an arrangement between global handling qualities of the entire concept and aerodynamic performances of each component like rotor, wing, and airframe. This arrangement allows tilt-rotors having the best aerodynamic

performance in each parametric flight conditions: take-off and landing in hovering flight, transition flight and cruise flight.

First, experimental and numerical research works have aimed at developing and modelling the flow aerodynamic characteristics generated by the rotor operating in an isolated configuration [2-5]. These studies have focused on the rotor wake evolution (vortices localization and intensity, age of vortices) in order to allow the validation of wake numerical models which are implemented in aero-acoustic codes. However, the study of aerodynamic interactions between the rotor and its nearest environment during different flight configurations can not only be done by studying each component separately. Actually, the wing placed directly in the rotor wake influences rotor aerodynamic performance. Thus, mutual aerodynamic influences of rotor and wing are very important in different flight configurations and this topic has already been studied.

In recent years, significant progresses have been done in the aerodynamic performance prediction of tilt-rotor blades operating at different flight conditions. However, detailed experimental databases are still needed to improve and validate CFD methods for example. Indeed, flow features around tilt-rotor blades are subject to aerodynamic interactions between the rotor, the nacelle and the fixed wing directly placed in the wake and are shown to be strongly dependent on the different flight conditions. Felker and Light [6] have studied such interactions exhibiting a download phenomenon on the wing in hovering flight. Later, Matos et al. [7] have also quantified this download behavior for different flap angle values on the wing. Young et al. [8] have shown that the wing download is generated at the root of the wing and extends along the span. Moreover, by means of pressure coefficients integrations, they have shown that the wing download (DL/C_T) was nearly equal to 0.105 which is a value very close to those of Felker et al. [9] and McVeigh et al. [10]. It has also been demonstrated in previous works that the airframe contribution to total download is very important in the hovering flight configuration. This is in accordance with the value of about 40% of total download measured by Wood and Peryea [11]. More recent studies [12] have quantified the aerodynamic interactions thanks to improvements in aircraft design. But they also reveal that a better understanding of the rotor wake evolution seems to be required in order to reduce aerodynamic interaction effects for a given tilt-rotor aircraft geometry. In addition to this, it should be considered that tilt-rotor blades aerodynamics is generally fundamentally different from helicopter ones. In such a way, tilt-rotor wake modeling should be strongly improved by means of suited experimental data providing a better understanding of vortex dynamics as recently studied by Richard [13] for helicopters rotor in a forward flight configuration.

For hovering flight conditions, Meakin [14] developed a Navier-Stokes code around moving body to model the flow on a V-22 tilt-rotor in the presence of a half span wing below it. However the Figure of Merit (FM) was quite under-predicted when compared to experimental data which have been obtained by Felker et al. [9]. One of the most efficient modeling improvements was made by Johnson [15] who developed the numerical tool called CAMRAD II. This last one is based on the second order of the lifting line theory and uses a vortex wake model to calculate induced velocities. Nevertheless, global and local aerodynamic performances are shown to be more and more dependent on the accuracy of the wake evolution and explain the fact that a lot of research works have been recently done for accurately modeling the rotor wake distortion due to the wing presence.

For cruise flight conditions, Johnson [16] has compared the influence of two different wake models which take into account the delay of the boundary layer separation on blade inboard sections due to centrifugal effects as observed by Barla et al. [17] on a V-22 tilt-rotor blade: a

simple rolled-up wake model (RUWM) where the formation of the tip vortex is the same as for a helicopter blade and a multiple trailer wake model (MTWM), where the viscous effects are not taken into account but coupled with a wake model in order to better estimate the vortex path. MTWM is shown to provide better correlations with experiments than RUWM, and to predict more accurately the vorticity field for low thrust coefficients. The results concerning lower thrust coefficients have also been studied by Yamauchi et al. [18] by means of 2C PIV measurements. This experiment constitutes one of the first wake vortices measurements in the airplane mode on a tilt-rotor configuration. Results specially show that tangential velocity component in the vortex core was proportional to the vortex size.

It is worth noting that there exists a relatively poor literature concerning detailed studies of the transition and/or conversion flight configurations. Indeed, almost all works attempt to develop and validate numerical models in order to gain insight in simple flight configurations. Therefore, it will be a challenge from now on to investigate such flight configurations which involve more complex parametric conditions and flow features.

In order to validate all these studies, LABM has developed experimental tools in the fields of propeller wake and wing aerodynamic interactions and also in rotors operating in an isolated configuration for different flight parametric conditions [19-22]. Now, these tools allow studying aerodynamic interactions from rotor on wing (and reciprocally) as a function of different geometric and aerodynamic flight parameters such as rotor shaft angle β, advance ratio $\mu=U_\infty/\Omega R$, wing incidence angle α or blade collective pitch angle θ.

The paper successively presents the tilt-rotor geometry and the flight parametric conditions relative to the present study. A detailed description of experimental tools developed to study aerodynamic interactions will be presented and some typical results like rotor and wing performance for different flight configurations will be given in the last part.

2 EXPERIMENTAL TEST SET-UP

Experiments have been performed on a 1/7 scaled tilt-rotor model set-up in the LABM S1L wind-tunnel as shown in Figure 1. The rotor is mounted in the V1 wind-tunnel test section (3m in diameter, 6m in length, maximum velocity 100 ms^{-1}) by means of a vertical cylindrical mast which can be rotated by a shaft angle β, with an accuracy of 0.025deg in the direction of the upstream velocity, in order to simulate the hovering flight (corresponding to $\beta=90°$ in figure 3a), the conversion (corresponding to $\beta=45°$ in figure 3b) and the cruise (corresponding to $\beta=0°$ in figure 3c).

2.1 Rotor and Blade Geometries

The set-up also includes a fixed wing in the rotor wake as well as an end plane plate simulating the airframe (2m*2m*0.25m). The wing is maintained in the test section by a secondary rotating mast which is mounted on the upper part of the wind-tunnel test section. The wing has a span h=0.770m, a chord c=0.31m and is equipped with an OACV23 airfoil profile. A flap angle value δ can be adjusted at 0deg or 50deg.

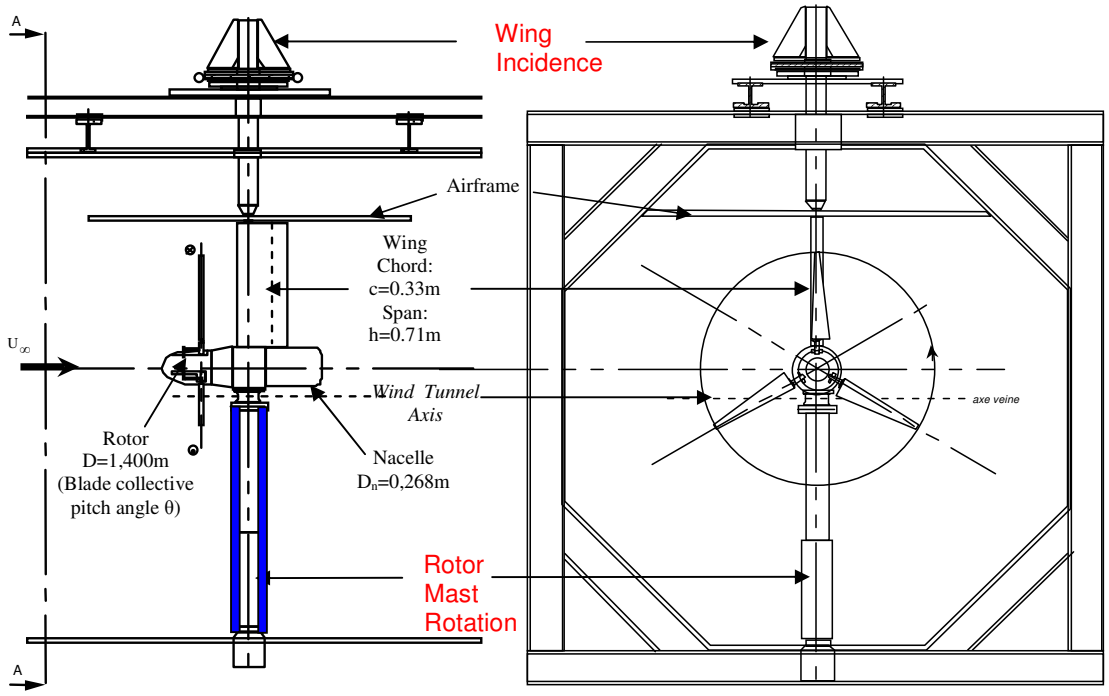

a) Front View b) Side View

Figure 1: Sketch of the tilt-rotor configuration.

The rotor (diameter D=0.140m and hub diameter D_0=0.27m) is fully articulated and equipped with a nacelle and 3 blades having non linear twist and chord laws and 3 different airfoil profiles along the blade span (OH120, OA312 and OA309). The planform of the LABM blade is shown in Figure 2 and is based upon EUROFAR blade geometry [23].

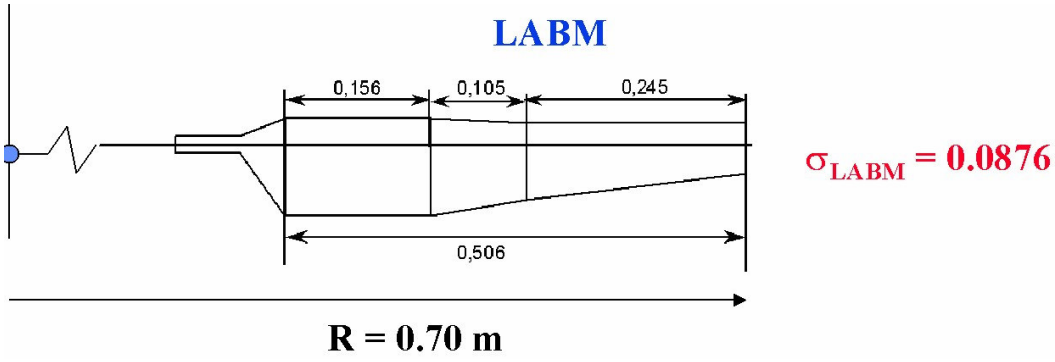

Figure 2: Blade planform

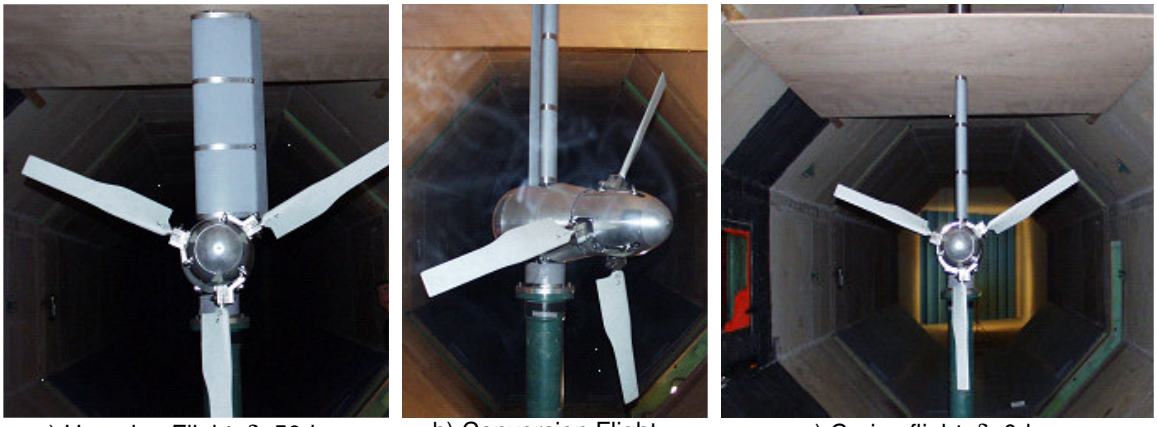

a) Hovering Flight, δ=50deg

b) Conversion Flight, δ=50deg

c) Cruise flight, δ=0deg

Figure 3: Views of the tilt-rotor set-up in different flight configurations

2.2 Global Performance Measurements

Global performance are measured using strain gauges settings which have been implemented on each supporting mast of the rotor and the wing. These masts are subject to elastic deformations during the different flight configurations and it causes resistance variations for each constraint gauge. Thus, via mechanical and electrical analyzes, the mechanical tensor is calculated thanks to the settings of 3 groups of 4 gauges on each supporting mast.

Concerning the rotor mast, gauges are placed on the external part of the mast submitted to aerodynamic forces. As shown in blue color in Figure 1a, a 1mm cylindrical mast has been added in order to avoid taking into account the effects of freestream velocity on the gauges during experimentations. Thus, aerodynamic performance measurements are performed on both rotor and nacelle and after that on the nacelle without rotor blades. As a consequence, by operating a simple algebraic difference, aerodynamic performance of the blades are determined. It can be noticed that simultaneous measurements on both rotor/nacelle are realized with a maximal error of 0.5% for forces and less than 1.5% for torques. Concerning the wing mast, the 3 forces are measured with a maximal error less than 1%.

2.3 Blade Vortices Path

For a middle wake area or at a given distance from blades, hot wire probes are easy to be operate and allow quickly determining the blade tip vortices path. Indeed, the probe reacts instantaneously to velocities variations and the simple evolution study of the axial velocity signal on an oscilloscope is done to determine the crossing of a vortex. A DANTEC 55R53 crossed wire probe is used and linked to a DANTEC 56C16 deck measurement. Investigations all over the wake are realized thanks to a 3D displacement device.

Temporal and spatial coordinates (X_t, Y_t, Z_t, Ψ_t) of the tip vortex are recorded when it interacts with the probe. Thus, the oscilloscope gives a maximum peak tension for a specific couple of coordinates and then there is a characteristic change of sign on the voltage tension which accurately localizes the vortex center. The phase ψ_t is also recorded and corresponds to the phase shift between the synchronization top indicating the phase origin and the voltage peak. This ψ_t parameter thus represents the age of the vortex which is detected modulo $2\pi/3$ for a three bladed rotor. Due to the presence of the wing downstream the rotor, the wake is not symmetric oppositely to the isolated rotor and the determination of wake shear layer is a function of the azimuthal position of the emitting blade.

Thus, tip vortex localization in space and time (X_t, Y_t, Z_t, Ψ_t) is performed at different downstream distances from the rotor in order to establish a complete representation of wake geometry due to the presence of the wing. However, vortex trajectory measurements are limited in the X-direction as spatial and temporal instabilities are detected on oscilloscope signal. This instability phenomenon is due to the progressive loss of helicoïdal form of each vortex trajectory emitted from one azimuthal position. This is due both to the viscous diffusion and the vortex interaction with the wing.

2.4 Parametric flight conditions

Each flight configuration is studied for specific parameters which are summarized in Table 1. These parameters are representative of the tilt rotor evolution during the different flight configurations.

Table 1: Flight conditions

Parameter	Hover	Transition	Cruise
Nacelle Shaft Angle (β in deg)	0	45	0
Blade Collective Pitch angle (θ in deg)	$0<\theta<25$	$0<\theta<25$	$40<\theta<50$
Wing incidence (α in deg)	90	0	0
Wing Flap Angle (δ in deg)	(0; 50)	(0; 50)	0
Rotor frequency (N in Hz)	22.7	22.7	18.18
Free Stream Velocity (U_∞ in m/s)	0	30	46
Advance Ratio μ	-	0.3	0.55

3 RESULTS AND DISCUSSION

The model scale of the rotor with its nacelle is set-up on the hovering test rig of LABM (located in the servicing hall of the wind tunnel). The rotor is operating in hover with an induced flow blowing from the bottom to the top in order to minimize ground and recirculation effects. It can be noticed than the same mast and the same strain gauges as in wind tunnel measurements are set-up in order to validate the system by comparison to HOST code [24] predictions (obtained by ONERA). As shown in Figure 4a, representing the evolution of rotor lift coefficient Z_b as a function of collective pitch angle θ, there exists differences between measurements and calculations. The Z_b values from LABM are a little bit higher than ONERA calculated values, but the slopes are similar. On Figure 4b) is plotted the rotor FM as a function of rotor lift coefficient Z_b, for measured and calculated values. One can notice that the predicted FM_{max} is higher than the measured FM_{max} value, possibly due to some discrepancies between the theoretical design of the airfoils and the real shape of the blade. Nevertheless, the thrust of FM_{max} is similar between calculation and experiment (close to Z_b= 27) and the loss of FM during the tests occurs at the same thrust than in prediction (around Z_b = 31). So, these first measurements have been realized in order to validate the overall forces measurement device.

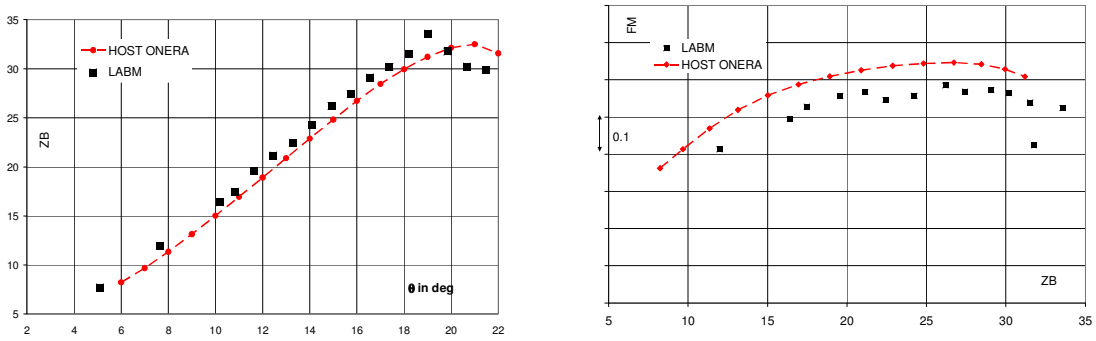

a) $Z_b = f(\theta)$ b) $C_T = f(C_Q)$

Figure 4: Comparisons of Global Performance in Hover (rotor outside wind-tunnel)

3.1 Hovering Flight

Two configurations have been considered with different parametric flight conditions summarized in Table 1: the first one is the rotor (R) equipped with its nacelle (N) and the airframe (A) called "isolated rotor" without the wing, and the second one which is the same as before with the presence of the wing (W) with 2 values of flapping angles. Figure 5 presents rotor lift coefficient Z_b as a function of collective pitch angle θ and rotor thrust coefficient C_T as a function of C_Q.

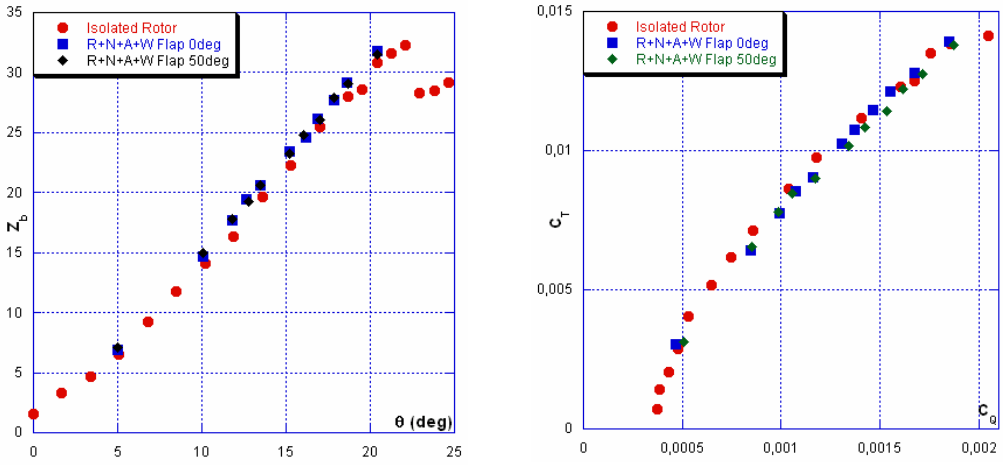

a) $Z_b = f(\theta)$ b) $C_T = f(C_Q)$

Figure 5: Global Performances on Rotor in Hovering Flight

Concerning the rotor lift coefficient, there is a little increase on Z_b for the same collective pitch angle if the flap of the wing is activated. It indicates that the presence of the wing allows obtaining a gain of traction for a same collective pitch angle. This gain is close to 5 % and is logically a bit higher with 0deg flap angle than with the 50deg flap angle, as shown in Figure 4a. This trend is also confirmed on the rotor thrust coefficient which exhibits small differences as shown in Figure 5b.

To study aerodynamic interactions, it is necessary to quantify the rotor impact on the wing aerodynamics thanks to a quantity called download which is given in Figure 6 for the 2 flap angle values. The result is in coherence with the literature, with a decrease of download for an increase of the flap angle value. For a 50deg flap angle, this decrease is about 40% compared

to a 0deg flap angle. Moreover, the download is relatively independent of the thrust values in this range of CT.

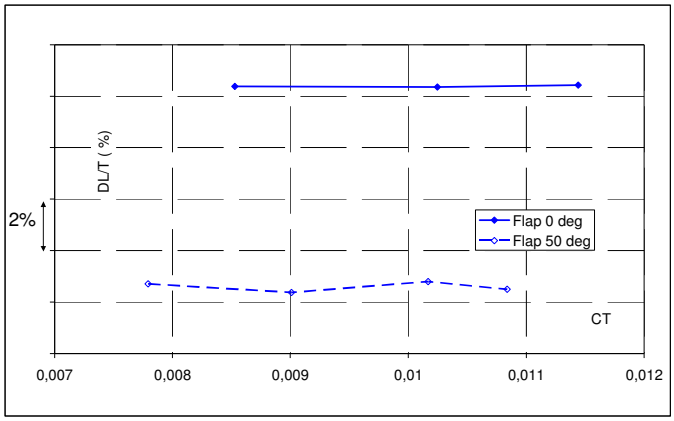

Figure 6: Download evolution with flap angle variations

3.2 Cruise Flight

For this flight configuration, the tilt-rotor behavior will be always considered with a flap angle equal to 0deg. First, the global performances on the rotor will be shown and then those on the wing. Figure 7 shows the evolution of rotor lift coefficient Z_b and the power evolution as a function of the collective pitch angle θ. Contrary to the hovering flight case, where a little gain of rotor lift was observed, the presence of the wing in the rotor wake has no noticeable influence as shown in Figure 7a. This was expected since the wing in cruise has almost 0deg incidence and thus does not influence the rotor thrust.

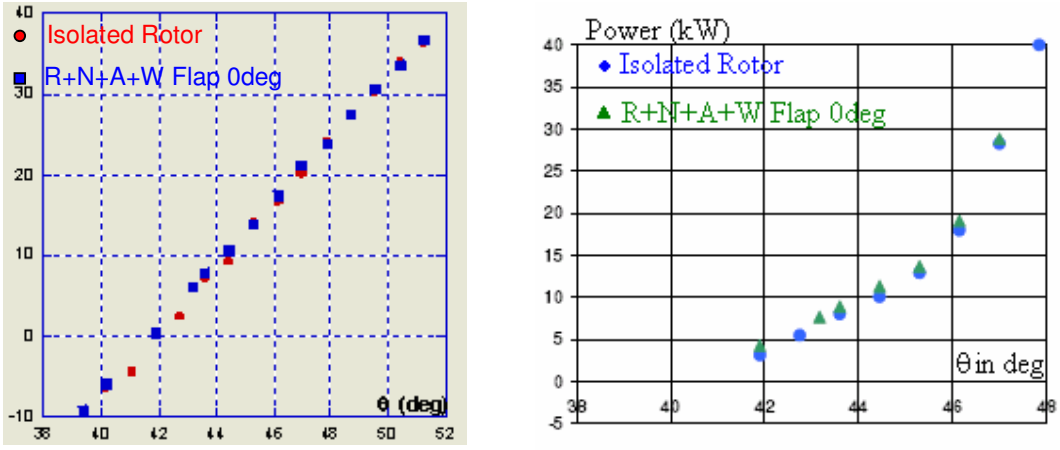

a) $Z_b = f(\theta)$ b) $P = f(\theta)$

Figure 7: Global Performance on Rotor in Cruise Flight Configuration

Considering the power evolution, it appears a little increase of power, around 3%, for the full model configuration compared to the isolated rotor. One can see that, above 46deg of collective pitch, the power strongly increases due to the too high incidence of the blade.

In order to study the influence of rotor on wing, aerodynamic coefficients of the wing have been measured for different configurations. First, the wing was placed in the wind tunnel between 2 end plates in order to simulate a 2D flow configuration; then, the end plate below the wing has been removed and finally the nacelle of the rotor has been placed just under the

wing tip (see Figure 1a) without the blade to identify the influence of the nacelle on the wing aerodynamic coefficients. Figure 8 shows the evolution of aerodynamic coefficients of the wing as a function of its angle of attack α.

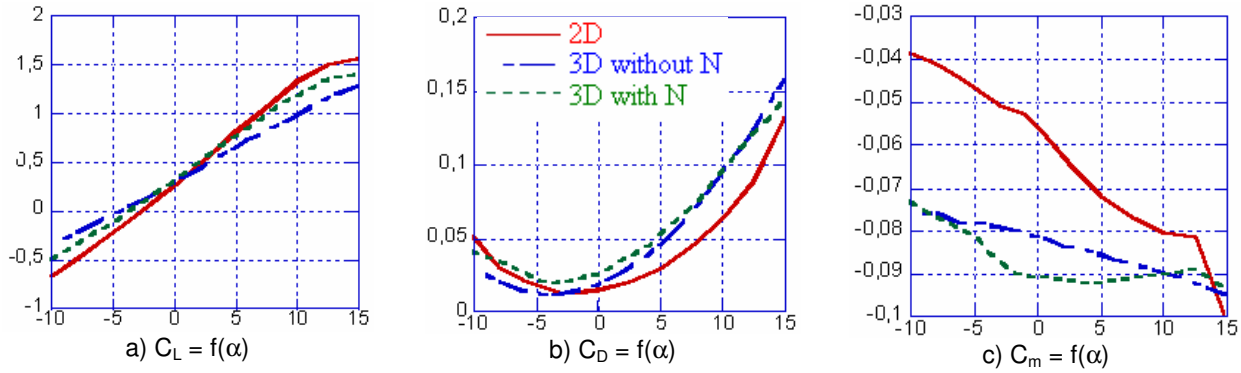

Figure 8: Aerodynamic coefficients of the wing for different steady configuration.

Aerodynamic coefficients have been measured for an angular variation of α comprised between -10deg and 15deg. Figure 8a gives the zero-lift α value for each configuration which are respectively -2.5deg for a 2D flow, -4deg for a 3D flow with nacelle and -5deg for a 3D flow without nacelle. The vortex formation at the tip of the wing creates an induced flow reducing the zero-lift α value. The presence of the nacelle in interaction with the wing tends to decrease the vortex influence for the lower lift coefficient. Furthermore, the slope of the C_L plot is shown to depend on the studied configuration. It reveals that the 3D flow configuration with the nacelle is the intermediate configuration for the C_L evolution. Figure 8b identifies the increasing level of C_D between a 3D and a 2D flow configuration. This increase clearly appears for positive values of wing incidence α, however, for negative values of α the free 3D flow configuration is higher than the 3D flow configuration without nacelle. Figure 8c shows higher nose-down effect on C_M coefficients for 3D configurations than for the 2D one. For each aerodynamic coefficient of the wing the 3D configuration without nacelle appears as an intermediate configuration between the two others.

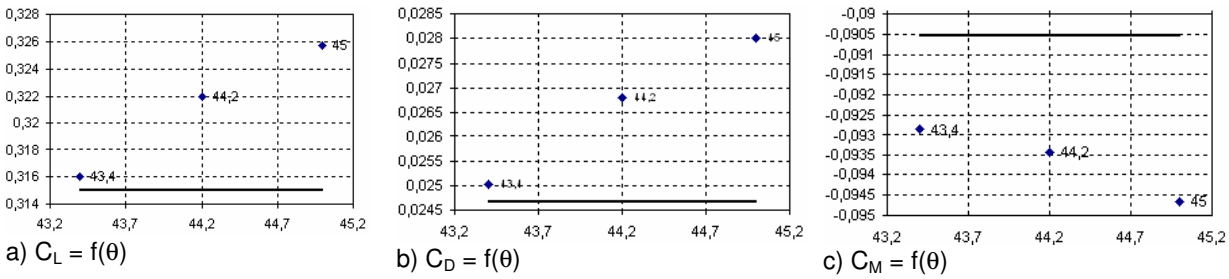

Figure 9: Aerodynamic coefficients of the wing for different unsteady configurations.

Figure 9 shows the influence of the blade rotation on the aerodynamic coefficients of the wing for a 3D flow configuration with the nacelle and for a zero α value. The black line respectively represents the (C_L, C_D, C_M) values obtained from Figure 7 for a zero α value. The three points characterizes the collective pitch angle θ increase for which different evolution concerning aerodynamic coefficients is shown. Figure 9a highlights a C_L upload phenomenon on the wing compared to the steady flow configuration as soon as the value of θ is higher than 43.4deg and this upload phenomenon induced a C_L increase of about 2% for θ=44.2deg. For the same conditions, Figure 9b and 9c quantify the effect of the blade rotation on the C_D and

C_M wing coefficients. It appears clearly that the aerodynamic coefficients behaviours are directly dependent on the collective pitch angle values. Indeed, the more the θ value is high, the more (C_L; C_D; C_M) differences with the steady flow configuration are high. This is due to the increase of the induced velocity level with the increasing collective pitch angle of blades.
The effect of the rotor thrust on the wing can also be noticed on the evolution of pressure coefficients Kp values: Figure 10 presents the difference of Kp, with and without rotor influence, on a wing section located inside the rotor wake. The pressure integration confirms the 2% increase of C_L for θ=44.2deg.

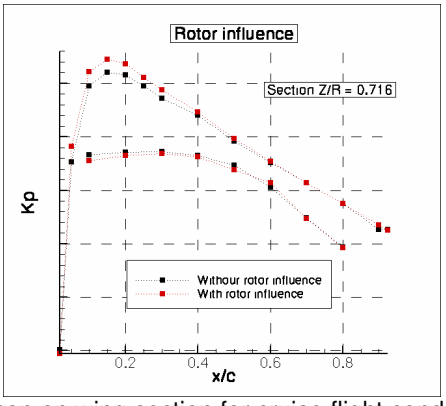

Figure 10: Kp comparison on wing section for cruise flight conditions

Hot wire probe measurements have also been performed at different downstream distances from the rotor and at different blade azimuth positions (ranging from ψ=0° in front of the wing leading edge to ψ=100°). The tip vortex paths have been reconstructed both in the wake region between the rotor and the wing and above the wing surface as shown in Figure 11 and Figure 12.

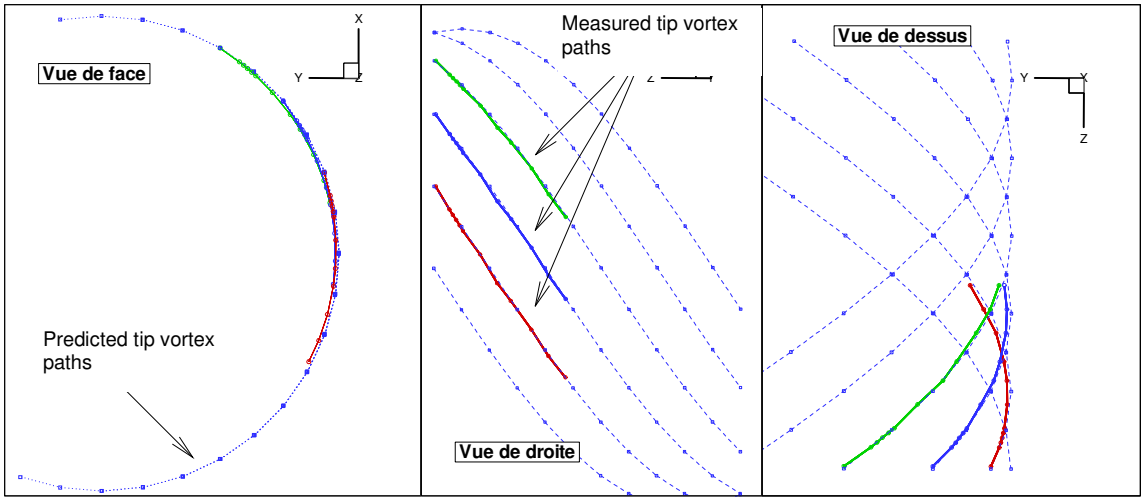

Figure 11: Predicted Tip Vortex paths (dotted lines) and measured Tip Vortex paths (full lines) for the isolated rotor wake in the cruise flight conditions

As an example, Figure 11 compares the tip vortex paths generated in the cruise flight conditions and measured during the Wind Tunnel tests to the predicted ones (obtained with HOST code), both for isolated rotor, for the same set of parametric flow conditions (f, U_∞, μ, θ). The result proves the very good accuracy of HOST prediction for this experimental configuration where the helical wake is not much distorted.

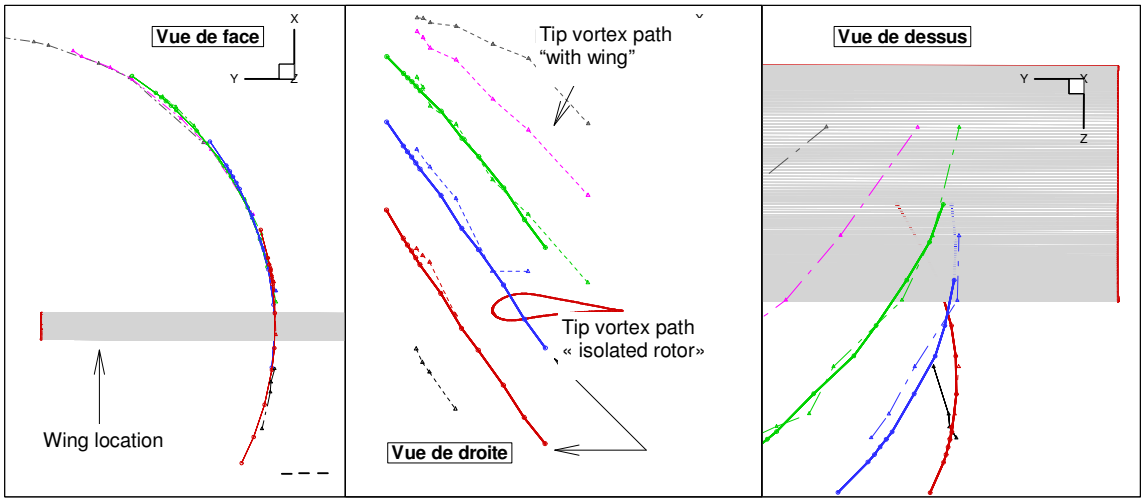

Figure 12: Tip Vortex paths in the isolated rotor wake (without wing, full lines) and in the cruise flight conditions (wing present, dotted lines)

Figure 12 shows the change occurring on the tip vortex paths which are generated in the same cruise flight configuration (but with the wing present), when compared to the vortex trajectories corresponding to the isolated rotor (without the wing). The results exhibit the wake geometry distortion due to the presence of the wing in the near wake: one can notice the increase of axial speed of the tip vortex when approaching the upper side of the wing (blue and green dotted lines) and a small decrease of axial speed in front of the wing (red dotted line).

4 CONCLUSIONS AND PERSPECTIVES

Several experimental methods have been developed and applied in the present study to a 1/7 tilt-rotor scale model operating in different flight configurations. Data concerning the rotor performance, the vertical wake and the wing aerodynamic behaviour have thus been obtained for investigating the aerodynamic interactions on a tilt-rotor operating in different flight configurations. In a next future, blade tip vortex paths will be investigated, by PIV, for different blade azimuth positions in order to improve understanding on the interaction phenomena. These measurements will be correlated with global performance in the conversion flight configuration. Thus, the wing download (respectively upload) phenomenon could be better estimated in hover or transition configurations (respectively cruise flight). Finally, such experimental databases will be used to improve numerical models of tilt-rotor wakes for different flight configurations.

5 ACKNOWLEDGEMENTS

The authors would like to acknowledge the French DPAC for funding the present study.

6 REFERENCES

[1] W. Johnson, "*Calculations of the Aerodynamic Behavior of the Tilt Rotor Aeroacoustic Model (TRAM) in the DNW*", Proceedings of the 57th AHS Annual Forum, Washington D.C., May 1999

[2] G.K. Yamauchi, C.L. Burley, E. Mercker, K. Pengel, R. Janakiram, "*Flow Measurements of an Isolated Model Tilt-rotor*", Proceedings of the 55th Annual Forum of American Helicopter Society, Montreal, Canada, 1999.
[3] M. Betzina, "*Rotor Performance of an Isolated Full-Scale XV-15 Tiltrotor in Helicopter Mode*", AHS, Aerodynamics, Acoustics, And Test And Evaluation Technical Specialists Meeting, San Francisco, Ca, January, 2002.
[4] D. Favier, A. Ettaouil, C. Maresca, "*Numerical and experimental investigation of isolated propeller wakes in axial flight*", Journal of Aircraft , Vol. 26, n° 9, 1989, pp. 837-846.
[5] W. Johnson, "*Airloads and Wake Geometry Calculations for an Isolated Tiltrotor Model in a Wind Tunnel*", Proceedings of the 27th European Rotorcraft Forum, Russia, September, 2001.
[6] F.F. Felker and J.S. Light, "*Aerodynamics Interactions Between a Rotor and Wing in Hover*", Journal of the American Helicopter Society, Vol.33, No.2, April 1988, pp 53.
[7] C. Matos, U. Reddy and N.K. Komerath, "*Rotor Wake/Fixed Wing Interactions with Flap Deflection*", Proceedings of the 55th Annual Forum of AHS, Montreal, Canada, May 1999.
[8] L.A. Young, D. Lillie, M. McCluer, G.K. Yamauchi, M.R. Derby, "*Insights into Airframe Aerodynamics and Rotor-on-Wing Interactions from a 0.25 Scale Tilt-rotor Wind Tunnel Model*", Proceedings of the American Helicopter Society International Aerodynamics, Acoustics, and Test and Evaluation Specialists' Conference, San Francisco, CA, January 2002.
[9] F.F. Felker, D. Signor, L.A. Young, M. Betzina, "*Performance and Loads Data from a Hover Test of a 0.658-Scale V-22 Rotor and Wing*", NASA TM 849419, 1987.
[10] M.A. McVeigh, W.K. Grauer, D.J. Paisley, "*Rotor/Airframe Interactions on Tilt-rotor Aircraft*", Journal of the American Helicopter Society, Vol. 35, N°3, June 1990, pp 43-51.
[11] T.L. Wood, M.A. Peryea, "*Reduction of Tilt-rotor Download*", Journal of the American Helicopter Society, Vol.40, N°5, July 1995, pp 42-51.
[12] W. Johnson, "*Calculations of TRAM Performance, Airloads and Structural Loads*", Proceedings of the American Helicopter Society Aeromechanics Specialists' Meeting, Atlanta, November 2000.
[13] H. Richard, "*Dynamique des tourbillons d'extrémité de pales de rotor en vol d'avancement*", Thèse de Doctorat de l'Université de la Méditerranée, 2005.
[14] R.L. Meakin, "*Unsteady Simulation of the flow about a V-22 Rotor and Wing in Hover*", AIAA Paper 95-3463, Proceedings of the Atmospheric Flight Mechanics Conference, August 1995, pp 332-344.
[15] W. Johnson, "*CAMRAD II, Comprehensive Analytical Model of Rotorcraft Aerodynamics and Dynamics*", Johnson Aeronautics, Palo Alto, 1992-1997.
[16] W. Johnson, "*Influence of Wake Models on Calculated Tilt-rotor Aerodynamics*", Proceedings of the 58th Annual Forum of American Helicopter Society, San Francisco, CA, January 2002.
[17] C. Barla, E. Berton, D. Favier, C. Maresca, "*Boundary Layer Investigation on a tilt-rotor blade by means of an Embedded Laser Doppler Velocimetry*", Journal of Aircraft, in press.
[18] G.K. Yamauchi, C.L. Burley, E. Mercker, K. Pengel, R. Janakiram, "*Flow Measurements of an Isolated Model Tilt-rotor*", Proceedings of the 55th Annual Forum of American Helicopter Society, Montreal, Canada, 1999.
[19] D. Favier, M. Nsi Mba, C. Barbi, C. Maresca, "*A free wake analysis for hovering rotors and advancing propellers*", Vertica, Vol. 11, n° 3, 1987, pp. 493-511.
[20] R. Muller, M. Nsi Mba, E. Aymard, D. Favier, E. Berton, C. Maresca, "*Visualization*

and measurement of helicopter rotor flow with swept back tip shapes at hover flight", Experiments in Fluids, Vol. 21, 1996, pp. 161-169.

[21] T. Berenger, D. Favier, C. Maresca, E. Berton, "*Experimental and Numerical Investigation of Rotor Aerodynamics in Forward Flight*", Journal of Aircraft, Vol.34, n°3, 1997, pp. 394-399.

[22] D. Favier, C. Maresca, M. Nsi Mba, E. Berton, A. Agnès, "*New Type of Embedded Laser Doppler Velocimeter (ELDV) for Measurements of Rotary Wings Boundary-Layer*", The Review of Scientific Instruments, Vol. 66, n° 6, 1997, pp. 2447-2455.

[23] B. Benoit, J.M. Bousquet, " *Aerodynamic design of a tilt-rotor blade*", 17th ICAS Congress, Stockholm (Sweden), September 9-14, 1990

[24] B. Benoit, A.-M. Dequin, K. Kampa, W. Grunhagen, P.-M. Basset, B. Gimonet, "*HOST, A General Helicopter Simulation, Tool for Germany and France*", 56th Annual Forum of the American Helicopter Society, Virginia Beach (USA), May 2002